ELSEVIER

Catalysis Today 81 (2003) 87–94

CATALYSIS TODAY

www.elsevier.com/locate/cattod

The selective oxidation of propane on Mo-V-Te-Nb-O catalysts The influence of Te-precursor

J.M. López Nieto*, P. Botella, B. Solsona, J.M. Oliver

Instituto de Tecnología Química, UPV-CSIC, Avenida de los Naranjos s/n, 46022 Valencia, Spain

Abstract

Mo-V-Te-Nb-O catalysts have been prepared by hydrothermal synthesis and have been tested in the selective oxidation of propane to acrylic acid. The catalysts have been prepared by using different Te- and Mo-starting compounds. Both the catalyst characterization results (XRD, SEM–EDX, FTIR and XPS) and the catalytic tests show important differences depending on the Te- and Mo-starting compounds used in the hydrothermal synthesis. The most active and selective catalysts for the oxidation of propane to acrylic acid were those prepared from Te(VI)-compounds, i.e. telluric acid or an Anderson-type telluromolybdate. However, catalysts prepared from Te(IV)-compounds, i.e. TeO_2 or $(NH_4)_4TeMo_6O_{22}\cdot 2H_2O$, presented both low activity and low selectivity to acrylic acid. In the best catalysts, several crystalline phases were observed: Mo_5TeO_{16}, $(Mo_{0.93}V_{0.07})_5O_{14}$, and/or $Nb_{0.09}Mo_{0.91}O_{2.80}$ and new Te-V-Nb-Mo-oxide crystalline phases. The presence of small crystals of MoO_3 in active and selective catalysts can also be proposed. The different catalytic performance of these catalysts could be related to the different incorporation of Te, V and Nb ions, which depends strongly on the Te-compound introduced in the synthesis gel.

Keywords: Selective oxidation of propane to acrylic acid; Mo-V-Te-Nb mixed oxide catalyst; Hydrothermal synthesis; X-ray diffraction; Diffuse reflectance UV-Vis; FTIR; SEM–EDX

1. Introduction

Mo-V-Te-Nb-O catalysts have been proposed as selective catalysts for oxidation [1] and ammoxidation [2] of propane. Recently, they have been proposed as active and selective in the oxidative dehydrogenation of ethane to ethylene [3,4]. The catalytic behavior of these materials has been related to the presence of two or more moieties, which should correspond to the presence of different crystalline phases [5–16]. However, the preparation method and the composition of the catalysts influence strongly both the nature of crystalline phases and their catalytic performance [1–16].

Although the slurry method is mainly used [1–3,5–8], hydrothermal synthesis has been recently proposed [3,4,9–12]. Ueda and Oshihara [9] reported the catalytic behavior for propane oxidation of Mo-V-Te-O catalysts prepared by hydrothermal synthesis using TeO_2 as starting compound. In this case, yields of acrylic acid of 12.4% were reported.

Recently, it has been reported the hydrothermal synthesis of an active and selective Mo-V-Te-Nb-O catalyst which presents an efficiency during the oxidation of propane to acrylic acid higher than the corresponding Nb-free catalyst [10,11]. In this case, an Anderson-type hexamolybdotellurate was used as Te-starting compound and a yield of acrylic acid of 35% was reported [11].

Mo-Te-V-Nb-O catalysts prepared by hydrothermal synthesis have also been reported as selective in the

* Corresponding author. Tel.: +34-96-38-77-808; fax: +34-96-38-77-809.
E-mail address: jmlopez@itq.upv.es (J.M. López Nieto).

0920-5861/03/$ – see front matter © 2003 Elsevier Science B.V. All rights reserved.
doi:10.1016/S0920-5861(03)00119-6

ammoxidation of propane to acrylonitrile [12]. However, no important differences in their catalytic performances between catalysts prepared from telluromolybdate or from TeO_2 were observed.

In this paper, we present the preparation, characterization and catalytic behavior of hydrothermally synthesised Mo-V-Te-Nb-O catalysts, in which different Mo- and Te-compounds have been used as starting materials. The results obtained here should show how both the catalytic behavior and physico-chemical properties of these catalysts depend strongly on the type of Te-compounds used in the hydrothermal synthesis.

2. Experimental

2.1. Catalyst preparation

Mo-V-Te-Nb-O catalysts have been prepared by a hydrothermal method according to the procedure previously reported [11]. The gel, an aqueous solution of the corresponding salts, presented a Mo-V-Te-Nb atomic ratio of 1-0.36-0.17-0.12. The gels were autoclaved in Teflon-lined stainless-steel autoclaves at 175 °C for 48 h. The resulting precursors were filtered, washed, dried at 80 °C for 16 h and heat-treated at 600 °C during 2 h in N_2-stream.

Vanadyl sulphate and niobium oxalate were used as V- and Nb-precursors. However, different Mo- and Te-compounds have been used:

- *Cat-**A***: A Te(VI)-containing ammonium hexamolybdotellurate, $(NH_4)_6TeMo_6O_{24}{\cdot}7H_2O$, was used as the Mo/Te-precursor. $(NH_4)_6TeMo_6O_{24}{\cdot}7H_2O$ was previously prepared according to a reported method [11,17,18].
- *Cat-**B***: A Te(IV)-containing ammonium hexamolybdotellurate, $(NH_4)_4TeMo_6O_{22}{\cdot}2H_2O$, was used as the Mo/Te-precursor. $(NH_4)_4TeMo_6O_{22}{\cdot}2H_2O$ was prepared according to the method reported previously [18,19].
- *Cat-**C***: Ammonium heptamolybdate and telluric acid were used as Mo- and Te-precursors, respectively.
- *Cat-**D***: Ammonium heptamolybdate and tellurium dioxide were used as Mo- and Te-precursors, respectively.

The characteristics of catalysts are shown in Table 1.

2.2. Catalyst characterization

X-ray diffraction patterns (XRD) were collected using a Philips X'Pert diffractometer equipped with a graphite monochromator, operating at 40 kV and 45 mA and employing nickel-filtered Cu Kα radiation ($\lambda = 0.1542$ nm).

The infrared spectra were recorded at room temperature on a NICOLET 710 FTIR spectrometer equipped with a Data Station. Twenty milligrams of dried samples were mixed with 100 mg of dry KBr and pressed into a disk (600 kg cm^{-2}).

Diffuse reflectance UV-Vis spectra (DRS) were collected on a Cary 5 apparatus equipped with a 'Praying Mantis' attachment (from Harric) under ambient conditions.

Scanning electron microscopy (SEM) and EDX microanalyses were performed on a JEOL JSM 6300 LINK ISIS instrument. The quantitative EDX analysis

Table 1
Characteristics of Mo-V-Te-Nb-O catalysts

Sample	Te source	S_{BET} ($m^2\ g^{-1}$)	Bulk composition[a] (Mo-Te-V-Nb)	UV-Vis bands (nm)	XRD crystalline phases
Cat-**A**	$(NH_4)_6Mo_6TeO_{24}.nH_2O$	9.1	1-0.12-0.18-0.19	320, 580	$TeMo_5O_{16}$; $Mo_{5-x}A_xO_{14}$[b]; **TeMO**[c]; MoO_3[d]
Cat-**B**	$(NH_4)_4Mo_6TeO_{22}{\cdot}4H_2O$	24.1	1-0.13-0.15-0.21	290, 580	$TeMo_5O_{16}$; $TeMo_4O_{13}$; **TeMO**[c]
Cat-**C**	H_6TeO_6	15.3	1-0.13-0.18-0.12	237, 305, 580	$TeMo_5O_{16}$; $Mo_{5-x}A_xO_{14}$[b]; **TeMO**[c]; MoO_3[d]
Cat-**D**	TeO_2	10.2	1-0.24-0.19-0.19	250, 313, 352, 580	$TeMo_5O_{16}$; $Mo_{5-x}A_xO_{14}$[b]; **TeMO**[c]

[a] The chemical composition has been determined by atomic absorption spectroscopy.
[b] $Mo_{5-x}A_xO_{14}$ with A = V and/or Nb.
[c] **TeMO** (M = Mo, V and Nb) as indicated in [13,16].
[d] The presence of a Mo-V-Te-Nb-O crystalline phase, M2-phase recently proposed by Millet et al. [16], should also be considered.

was performed using an Oxford LINK ISIS System with the SEMQUANT program, which introduces the ZAF correction.

2.3. Catalytic tests

The catalytic experiments were carried out in a tubular flow reactor at atmospheric pressure. The flow rate (from 50 to 200 $cm^3\ min^{-1}$) and the amount of catalyst (from 0.5 to 3.0 g) were varied in order to achieve different propane conversion levels. The feed consisted of a mixture of propane/oxygen/water/helium with a molar ratio of 4/8/30/58. Experiments were carried out in the 340–400 °C temperature range. Reagents and reaction products were analysed by on-line gas chromatography; further details on the method of analysis and on the reactor are reported elsewhere [11].

3. Results and discussion

3.1. Catalyst characterization

Fig. 1 shows the XRD patterns of catalysts. Different crystalline phases are observed depending on the Mo/Te-starting materials. The XRD pattern of sample Cat-**A** shows the presence of $TeMo_5O_{16}$ [JCPDS, 31-874], $Nb_{0.09}Mo_{0.91}O_{2.80}$ [JCPDS, 27-1310] and/or $(Mo_{0.93}V_{0.07})_5O_{14}$ [JCPDS, 31-1437], and MoO_3 [JCPDS, 5-508]. On the other hand, the presence of a Mo-V-Te-Nb-O crystalline phase (which crystallize in the orthorombic system [16]) should also be considered.

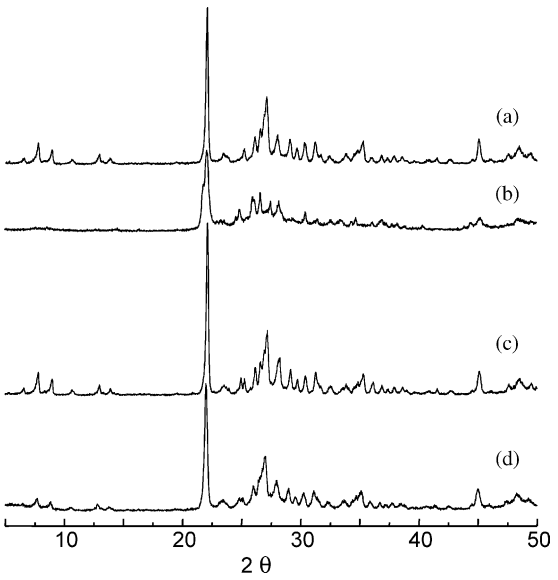

Fig. 1. XRD patterns of Mo-V-Te-Nb-O catalysts: Cat-**A** (a); Cat-**B** (b); Cat-**C** (c); and Cat-**D** (d).

In addition, the presence of peaks at 2θ = 22.1, 28.2, 36.2, 45.2, and 50.0 suggests the formation of a recently reported Te-V-Mo-O or Te-V-Nb-Mo-O (**TeMO**) crystalline phase [13,14]. These **TeMO** phases, with a stoichiometry of $Te_{0.33}Mo_{0.75}V_{0.25-x}Nb_xO_z$ ($0 < x < 0.25$), present XRD patterns similar to those observed in hexagonal tungsten bronze ($K_{0.13-0.33}WO_3$) or $Sb_{0.4}MoO_{3.1}$ [14] and could correspond to the phase-M2 proposed by Ushikubo et al. [5] and to the phase-M1 proposed by Aouine and Dubois [15].

Similar crystalline phases than those observed in sample Cat-**A** have been observed in Cat-**C** and Cat-**D** (Fig. 1c and d, respectively), although the intensities of the most important reflections were lower in the case of sample Cat-**D**.

A different XRD pattern was observed for sample Cat-**B**. In fact, the presence of two peaks at 21.8 and 22.2 suggests the presence of both $TeMo_5O_{16}$ and $TeMo_4O_{13}$ [JCPDS, 34-622]. However, the absence of peaks in the low 2θ interval indicates the absence of $(Mo_{0.93}V_{0.07})_5O_{14}$ and/or $Nb_{0.09}Mo_{0.91}O_{2.80}$. No formation of MoO_3 was observed in this case.

Fig. 2 shows the SEM micrographs of samples Cat-**A** (Fig. 2a) and Cat-**D** (Fig. 2b). Similar micrographs were obtained in the other samples. The SEM images of these samples are characterised by the presence of small slabs of less than 1 μm diameter. On the other hand, the global compositions obtained by EDX were in good agreement with those obtained by AAS (Table 1). Besides the global composition, the SEM–EDX analysis evidences a high homogeneity in the composition of the different particles. Thus, Mo-Te-V-Nb molar ratios of 1/0.26-0.33/0.18-0.47/0.10-0.11 and 1/0.09-0.18/0.27-0.34/0.11-0.14 were clearly observed in SEM–EDX analysis of particles in both Cat-**A** and Cat-**C**. However, Mo-Te-V-Nb molar ratios of 1/0.09-0.21/0.10-0.19/0.20-0.28 were mainly observed in the case of samples Cat-**B** and Cat-**D**.

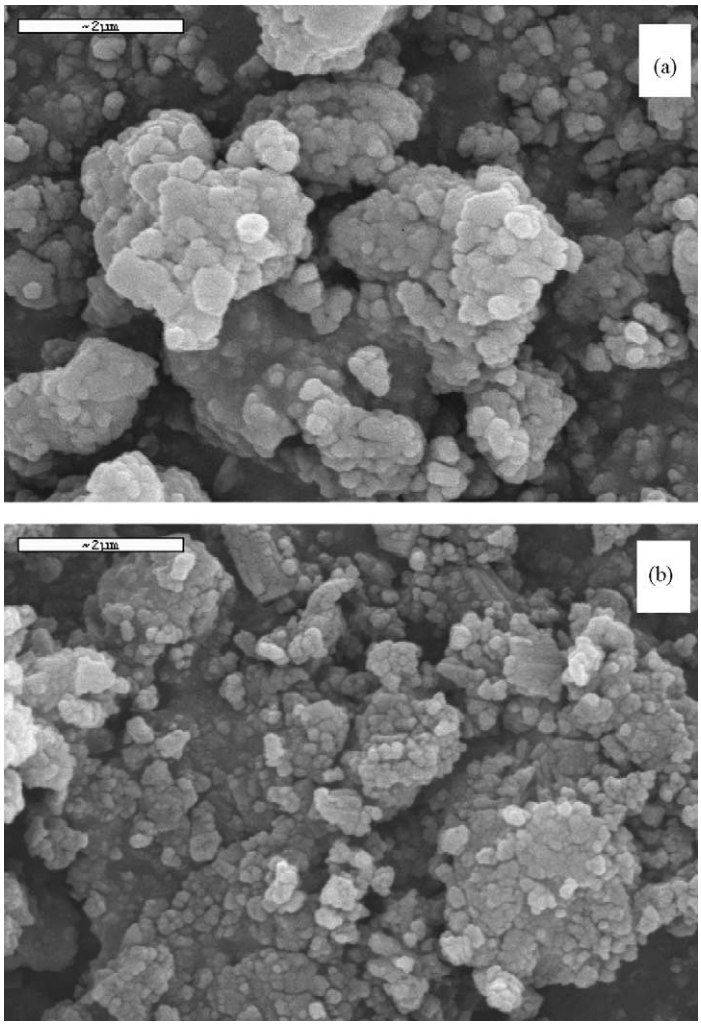

Fig. 2. SEM micrographs of samples: Cat-**A** (a); and Cat-**D** (b).

The FTIR spectra of catalysts in the low wavenumber region are shown in Fig. 3. Bands at 902, 880 (a shoulder), 790, 770, 632 and 586 cm^{-1} have been observed in the IR spectrum of sample Cat-**A**. These bands could be related to the symmetric stretching vibration of Mo=O group (bands in the 900–1000 cm^{-1}) and to antisymmetric vibrations of Mo-O-Me (Me = Mo, Nb, Te) bridging bonds (bands in the 700–900 cm^{-1}) [18,20]. On the other hand, the band at 632 cm^{-1} could be related to the presence of Te–O bonds [18,20]. Small differences are observed in the spectra of sample Cat-**C** and Cat-**D**.

The spectrum of sample Cat-**B** is quite different to those obtained with the other samples. Thus, a broad band is observed in the 920–870 cm^{-1} interval, while the bands at 775 and 620 cm^{-1}, observed in other cases, present low intensities (Fig. 3b). These results suggest, in agreement to the XRD results, that different crystalline phases are formed in this case.

On the other hand, the presence of MoO_3 (band at 991 cm^{-1}) is not observed in Cat-**B**. However, this band is present, although with low intensity, in the IR spectra of samples Cat-**A**, Cat-**C** and Cat-**D**.

Fig. 4 shows the DRS spectra of Mo-V-Te-Nb-O catalysts. For comparison purpose, different reference

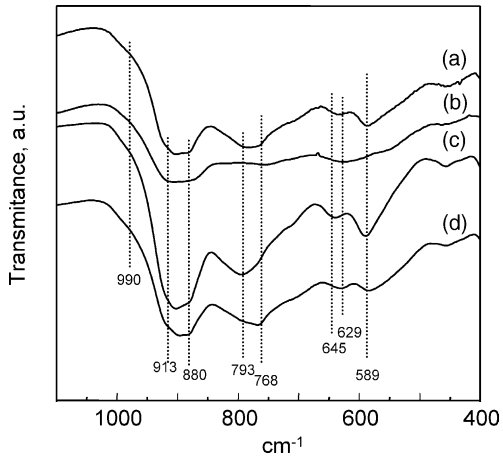

Fig. 3. FTIR spectra of Mo-V-Te-Nb-O catalysts: Cat-**A** (a); Cat-**B** (b); Cat-**C** (c); and Cat-**D** (d).

compounds such as $TeMo_5O_{16}$ (bands at 262, 355 and 550 nm) MoO_3 (bands at 250 and 314 nm), Nb_2O_5 (bands at 266 and 327 nm), MgV_2O_6 (bands at 257, 366 nm) and TeO_2 (bands at 245 and 289 nm) have been used (Fig. 5).

The DRS spectra of Mo-V-Te-Nb-O catalysts are characterised by the presence of two type of bands: (i)

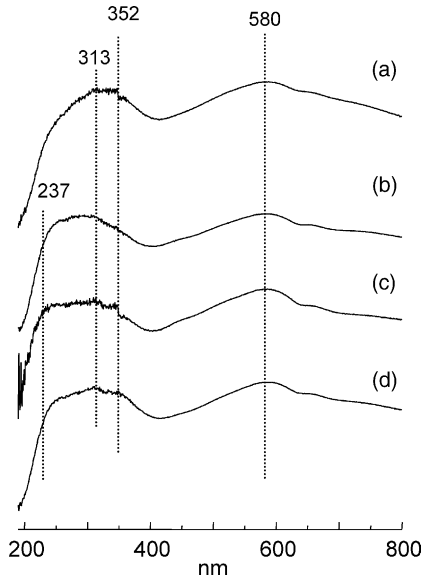

Fig. 4. DRS (UV-Vis) spectra of Mo-V-Te-Nb-O catalysts: Cat-**A** (a); Cat-**B** (b); Cat-**C** (c); and Cat-**D** (d).

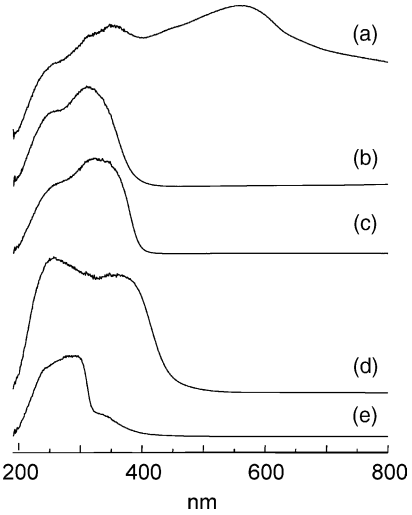

Fig. 5. DRS (UV-Vis) spectra of: $TeMo_5O_{16}$ (a); MoO_3 (b); Nb_2O_5 (c); MgV_2O_6 (d); TeO_2 (e).

a broad band in the range 250–400 nm which changes with the characteristics of catalysts; and (ii) a broad band centered at 580 nm similar in all catalysts.

The broad band in the 250–400 nm region is related to the presence of Mo^{6+} [21,22] and V^{5+} [22,23], although their positions depend on the Me-environment. The absorption bands in the range 290–350 and 350–450 nm can be related to the presence of Mo^{6+} and V^{5+} cations, respectively, in octahedral environment. According to previous results [10,11], molybdenum atoms in Mo-V-Te-Nb catalysts should posses a distorted six-coordinated environment with Mo^{6+}–O–Me bridges bonds (Me = Mo^{5+} and/or Mo^{6+}, in addition to V^{5+} and/or Nb^{5+}). So, the differences observed in the 250–400 nm region should be related to the different crystalline phases detected by XRD.

On the other hand, the band in the 500–600 nm region may be assigned to Mo cations with an oxidation state lower than 6+ [20–22,24]. It has been reported that MoO_2 present a band at 500 nm [24], while this appears at 550 nm in $TeMo_5O_{16}$ [20] and at 585 nm in Mo_9O_{26} [22]. Porter et al. [22] proposed a linear relation between the band frequencies observed in intermediate molybdenum oxides and the number of 4d electrons per cation. According with this, it could be estimated an oxidation state of molybdenum of 5.8 (suggesting the presence of a 20% of Mo atoms with

an oxidation state of Mo^{5+}) in our catalysts. This is in good agreement to previously reported EPR results of Mo-V-Te-Nb-O samples prepared by hydrothermal synthesis [10].

The presence of V^{4+} (broad band in the 600–750 nm region) cannot be completely ruled out. However, and according to previous EPR results [10], its presence, if any, should be very low.

The assignation of an oxidation state of the Te atoms from the DRS spectra represent some difficulties, since both Te^{4+} and Te^{6+} present bands in the range 250–300 nm. However, XPS results on similar catalysts suggest the presence of Te^{4+} ions [6,11]. This is also in good agreement to the oxidation state of Te in $TeMo_5O_{16}$ [20,24] and in related Mo-V-Te mixed oxide [9], and recently confirmed by ^{125}Te Mössbauer spectroscopy [16]. The formation of Te^{4+} from Te^{6+} compounds is generally accepted when the samples are heat-treated at high temperature [25].

From these results, it can be concluded that Mo^{6+}, Mo^{5+}, V^{5+} and Te^{4+} are mainly present in our catalysts.

3.2. Selective propane oxidation to acrylic acid

Table 2 shows the catalytic results obtained during the oxidation of propane. Acrylic acid, propene and carbon oxides were the main reaction products. Acetic acid was also observed, although the selectivity was lower than 10%. From these results, it can be concluded that the catalysts prepared from Te(VI)-containing compounds (samples Cat-**A** and Cat-**C**) are more active and selective than those prepared from Te(IV)-containing products (samples Cat-**B** and Cat-**D**).

Mo-Te mixed metal oxides catalysts, obtained by calcination of molybotellurates, have been recently reported as active and selective in the oxidation of propene to acrolein, specially those prepared from Te(IV)-molybotellurates [18]. However, the most effective Mo-V-Te-Nb-O catalysts were achieved from Te(VI)-containing precursors, although Te^{6+} is transformed to Te^{4+} during the heat-treatment at 600 °C in N_2. So, it seems that Te^{6+} is an important element to form active and selective crystalline phases precursors during the hydrothermal synthesis.

It has been proposed that the formation of crystalline phases in Nb-free Mo-V-Te-O catalysts prepared by hydrothermal synthesis takes place between molybotellurate units and vanadyl cations forming slabs and then being stacked to form a solid with layered structure [26]. According to our results, the incorporation of both vanadium and tellurium in the solids during the hydrothermal synthesis depends on the type of Te-precursor, which influences the nature of crystalline phases and the catalytic behavior in heat-treated samples.

The role of Nb in Mo-V-Te-Nb-O catalysts is still unclear. However, the presence of Nb favours both the achievement of higher surface areas [10] and higher selectivities to acrylic acid during the selective oxidation of propane or propene [11,13].

Table 2
Selective oxidation of propane on Mo-V-Te-Nb-O-based catalysts[a]

Sample	W/F[b]	Conversion (%)[c]	Yield AA (%)[d]	Selectivity (%)				
				CH_2CHCO_2H	C_3H_6	CH_3CO_2H	CO	CO_2
Cat-**A**	205	20.5	11.5	56.2	13.1	3.6	8.2	19.1
	510	36.9	19.9	54.0	5.7	3.6	11.2	25.5
Cat-**B**	205	17.0	0.6	3.8	9.3	3.7	27.0	56.0
Cat-**C**	205	30.6	17.1	56.0	13.6	5.9	8.8	15.7
	510	53.9	27.9	51.7	2.4	7.7	11.6	26.6
Cat-**D**	205	10.1	2.4	23.9	26.6	2.2	15.7	31.6

[a] Reaction temperature = 380 °C; C_3H_8-O_2-H_2O-He molar ratio of 4-8-30-58.
[b] Contact time, W/F, in $g_{cat}\,h\,(mol_{C_3})^{-1}$.
[c] Propane conversion in %.
[d] Yield of acrylic acid in %.

The catalytic activity could be related to the presence of $Nb_{0.09}Mo_{0.91}O_{2.80}$ and/or $(Mo_{0.93}V_{0.07})_5O_{14}$ (or to the formation of $Mo_{5-x}(V/Nb)_xO_{14}$) since they were not observed in the non-selective catalyst (Cat-**B**). Moreover, the possibility to have an active and selective Mo-V-Te-Nb crystalline phase, as proposed by Millet et al. [16], should also be considered. In this way, it has recently been proposed that V species are the active sites in alkane activation on Mo-V-Te-Nb-O catalysts [4,7–9] in the same way than that proposed in other V-containing catalysts [27–29].

On the other hand, small crystals of MoO_3 are observed on the selective catalysts. Although the role of MoO_3 is not clear in our case, it is known that its presence favours the selective oxidation of propene on Mo-based catalysts [18,30].

Fig. 6 shows the variation of the main reaction products with the propane conversion obtained on sample Cat-**C** at 380 °C. It can be seen that propene is a primary unstable product while carbon oxides are primary and secondary products. Acrylic acid could directly be formed from propane. However, our results suggest that it is mainly formed from propene. According to this, a reaction network for the oxidation of propane on these catalysts is tentatively proposed in Scheme 1. This is in good agreement to previously reported reaction networks [8,10,11,31,32].

The formation of propene and acrylic acid is the most important reaction. In addition to these, the formation of carbon oxides (by parallel and consecutive reaction) and the formation of acetic acid (from propene [10]) are also observed.

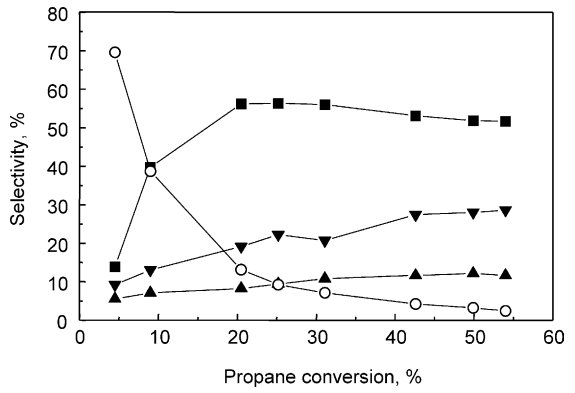

Fig. 6. Variation of the selectivity to the main reaction products with the propane conversion obtained on sample Cat-**C** at 380 °C: Propene (○); acrylic acid (■); CO (▲); and CO_2 (▼). Experimental conditions in text.

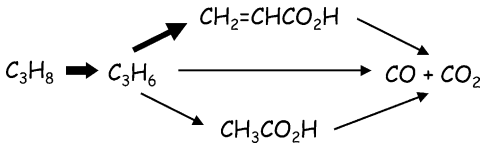

Scheme 1. Reaction network for the selective oxidation of propane on Mo-V-Te-Nb-O catalysts.

4. Conclusions

In conclusion, Mo-V-Te-Nb-O catalysts prepared by a hydrothermal synthesis are active and selective in the oxidation of propane to acrylic acid, although their catalytic behavior strongly depend on the Te-compounds used as precursors. High activity and selectivity to acrylic acid is observed on catalysts prepared from Te^{6+}-containing precursors, i.e. telluric acid or a Te(VI)-molybdotellurate. However, low capability in the formation of acrylic acid if any is observed when the catalysts are prepared from Te^{4+}-containing precursors, i.e. tellurium oxide (low activity and selectivity) or a Te(IV)-molybdotellurate (non-selective). Since Te^{4+} is mainly observed in calcined samples, it can be concluded that the formation of active and selective sites is favored by the use of Te^{6+}-containing precursors.

The dispersion of the active sites on the surface of the catalysts could be related to the characteristics of the solid obtained during the hydrothermal synthesis, which could be modified by tailoring the catalyst composition and/or the catalyst preparation method [1–13]. In this way, the results presented here suggest that the nature of the Te-compound precursors seems to have an important role in the preparation of selective Mo-V-Te-Nb-O catalysts. This could be related to a different incorporation of Te, V and Nb ions in the solids, as suggested from the EDX analysis.

On the other hand, it has been proposed that the activity of these catalysts in the propane activation is related to V^{5+} species [6,11,13]. Cat-**A** and Cat-**C** were the most active and selective catalysts, although they present V-contents similar to those obtained in samples Cat-**B** and Cat-**D**. So, the different

behavior of these catalysts should be related to the formation of different V-containing crystalline phases, which could present different activities in the alkane activation. Since, it has been observed that **TeMO** (M = Mo, V and Nb) crystalline phases are inactive in propane oxidation [13], the different catalytic activity of our catalysts could be related to the formation of $Mo_{5-x}(V/Nb)_xO_{14}$ and/or Te-containing Mo-V-Nb oxide [11,16]) which are not observed in the inactive catalyst (Cat-**B**).

Acknowledgements

Financial support from DGICYT, Spain (Project PPQ2000-1396) is gratefully acknowledged.

References

[1] T. Ushikubo, H. Nakamura, Y. Koyasu, S. Wajiki, US Patent 5,380,933 (1995), EP 0,608,838 B1 (1997).
[2] T. Ushikubo, I. Sawaki, K. Oshima, K. Inumaru, S. Kovayakawa, K. Kiyono, EP 0,603,836 (1993), US Patent 5,422,328 (1993).
[3] J.M. López Nieto, P. Botella, M.I. Vázquez, A. Dejoz, SP Patent, 1,104 (2002).
[4] J.M. López Nieto, P. Botella, M.I. Vázquez, A. Dejoz, Chem. Commun. (2002) 1906.
[5] T. Ushikubo, K. Oshima, A. Kayou, M. Hatano, Stud. Surf. Sci Catal. 112 (1997) 473.
[6] K. Asakura, K. Nakatani, T. Kubota, Y. Iwasawa, J. Catal. 194 (2000) 309.
[7] R.K. Grasselli, Top. Catal. 15 (2001) 93.
[8] M.M. Lin, Appl. Catal. A: Gen. 207 (2002) 1.
[9] W. Ueda, K. Oshihara, Appl. Catal. A: Gen. 200 (2000) 135.
[10] P. Botella, J.M. López Nieto, A. Martinez-Arias, B. Solsona, Catal. Lett. 74 (2001) 149.
[11] P. Botella, J.M. López Nieto, B. Solsona, A. Mifsud, F. Márquez, J. Catal. 209 (2002) 445.
[12] H. Watanabe, Y. Koyasu, Appl. Catal A: Gen. 194/195 (2000) 479.
[13] P. Botella, J.M. López Nieto, B. Solsona, Catal. Lett. 78 (2002) 383.
[14] E. Garcia-Gonzalez, J.M. López Nieto, P. Botella, J.M. Gonzalez-Calbet, Chem. Mater. 14 (2002) 4416.
[15] M. Aouine, J.L. Dubois, J.M.M. Millet, Chem. Commun. (2001) 1180.
[16] J.M.M. Millet, H. Roussel, A. Pigamo, J.L. Dubois, J.C. Jumas, Appl. Catal. A: Gen. 232 (2002) 77.
[17] I.L. Botto, C.I. Cabello, H.J. Thomas, Mater. Chem. Phys. 47 (1997) 37.
[18] P. Botella, J.M. López Nieto, B. Solsona, J. Mol. Catal. A: Chem. 184 (2002) 335.
[19] V. Balraj, K. Vidyasagar, Inorg. Chem. 38 (1999) 1394.
[20] J.C.J. Bart, F. Cariati, A. Sgamelloti, Inorg. Chim. Acta 36 (1979) 105.
[21] H. Aritani, T. Tanaka, T. Funabiki, S. Yoshida, K. Eda, N. Sotani, M. Kudo, S. Hasegawa, J. Phys. Chem. 100 (1996) 19495.
[22] V.R. Porter, W.B. White, R. Roy, J. Solid State Chem. 4 (1972) 250.
[23] T. Blasco, P. Concepción, J.M. López Nieto, J. Pérez-Pariente, J. Catal. 152 (1995) 1.
[24] J.C.J. Bart, G. Petrini, N. Giordano, Z. Anorg, Allg. Chem. 413 (1975) 180.
[25] F.J.J.G. Janssen, J. Thermal Anal. 87 (1991) 1281.
[26] K. Oshihara, T. Hisano, W. Ueda, Top. Catal. 15 (2001) 153.
[27] S. Alboneti, F. Cavani, F. Trifiró, Catal. Rev. Sci. Eng. 38 (1996) 413.
[28] T. Blasco, J.M. López Nieto, Appl. Catal. A: Gen. 157 (1997) 117.
[29] M.M. Bettahar, G. Costentin, L. Savary, J.C. Lavalley, Appl. Catal. A 145 (1996) 1.
[30] U.S. Ozkan, M.R. Smith, S.A. Driscoll, Stud. Surf. Sci. Catal. 72 (1992) 363.
[31] M. Lin, T.B. Desai, F.W. Kaiser, P.D. Klugherz, Catal. Today 61 (2000) 223.
[32] L. Luo, J.A. Labinger, M.E. Davis, J. Catal. 200 (2001) 222.